OPTIMIZING EXPERIMENTAL SETUP IN SIMULATED ORGANS FOR ULTRASOUND SYSTEMS

F. Conversano[1], S. Casciaro[1,2], R. Palmizio Errico[1], E. Casciaro[1,2], A. Distante[1,2]

[1] ISBEM Euro Mediterranean Biomedical Scientific Institute, Brindisi, Italy
[2] National Council of Research, Institute of Clinical Physiology, Lecce, Italy

conversano@isbem.it

Abstract: In recent years the knowledge of contrast agent (CA) behaviour in diagnostic ultrasound is continuously improving, mainly thanks to "in vitro" measurements performed by means of phantoms that aim to closely mimic acoustic properties of several human body districts without introducing any artefact. So it is evident the need to develop experimental setups able to minimize chemical and physical effects due to environmental conditions. In this work we discuss about the design of a new phantom, aiming in particular to evaluate the sound-absorption properties of three synthetic materials (Polyurethane, Airex© and ethylene vinyl acetate (EVA©)) laid on the bottom of the phantom. Our final goal is to establish which is the best material to use in order to minimize the artefact effects. This study was carried out by insonifying our tissue-mimicking phantom at different transmit frequencies, with the purpose of exploring each material suitability in a wide frequency range. Polyurethane showed the best sound-absorbant behaviour for every tested frequency, so its employment in covering the bottom of the phantom allows to minimize the artefacts and to investigate the backscatter properties of different CA without additional aspects due to environmental boundary conditions.

Introduction

In recent years, the knowledge of the behaviour of ultrasound (US) microbubble contrast agents (CA) has improved through in vitro experiments.

Various in vitro systems, both flowing and static, have been in fact developed [1-5] to evaluate microbubble acoustic behaviour. Flow phantoms in particular are designed to closely mimic flow in human vessels and, therefore, it is important that the acoustic properties of phantom components are very similar to those of the corresponding human tissues.

In this work we discuss about the design of a new phantom, developed and modulated in order to be able to study the US signal behaviour in almost all kind of human tissues, being also able to cover all vessel sizes and to reproduce the different vascular system conditions in terms of spatial and geometrical configuration.

Our specific aim, in this case, was the evaluation of the sound-absorption properties of three synthetic materials (Polyurethane, Airex© and ethylene vinyl acetate (EVA©)) laid on the bottom of the phantom, in order to establish which is the best material to use to minimize the artefact effects due to US reflections by static objects located below the phantom core.

To increase the reader's awareness of the discussed topic, we give a brief description of "sound-absorbant material" meaning and how the sound absorption phenomenon takes place.

Sound-absorbant materials are porous, with pore diameters belonging to the range between 2 and 5 μm. A large part of the incident acoustic wave penetrates the porous surface and the air molecules contained in the pores consequently start vibrating. Energy is dissipated by friction, air viscosity and heat transmission. The latter is a result of the compression and rarefaction of the air in pores. These materials have low densities, from 20 kg/m^{-3} to 200 kg/m^{-3} and they are often classified on the basis of their porosity, which is a dimensionless parameter defined as the ratio between the air volume included in the pores and the volume of the porous layer [6]. Polyurethane, Airex© and EVA© belong to this class of materials and we tested them by employing different US transmit frequencies, in order to explore the suitability of the studied materials in a wide frequency range.

Here we present a method to establish the optimal depth to place the vessel cavities in a new tissue-mimicking phantom, in order to minimize the influence exerted on CA measured signals by US reflected waves coming from the bottom of the phantom. The features of these "unwanted" signals, in particular their intensity at the various depths inside the phantom, strongly depend on the bottom material or on the employed sound-absorbant material.

Materials and Methods

The employed phantom was a custom-designed tissue-mimicking phantom consisting of a Plexiglas box (6 cm deep, 5 cm long and 8 cm wide) filled with an hydrogel having a sound propagation velocity (c=1559.5 m/s) very close to the corresponding human liver value (c=1560 m/s) [7]. Three different sound-absorbant strips (one for each tested material) were

ISSN: 1727-1983

aligned on the bottom of the Plexiglas box. All strips had the same thickness (a few millimeters) and the same width (approximately 2 cm).

A linear array US transducer (LA 523, Esaote Spa, Florence, Italy) was positioned on the top of the phantom using a coupling gel and a pair of clamps, so that the imaging plane resulted perpendicular to the materials on the bottom. A picture of the phantom coupled with the transducer is reported in figure 1.

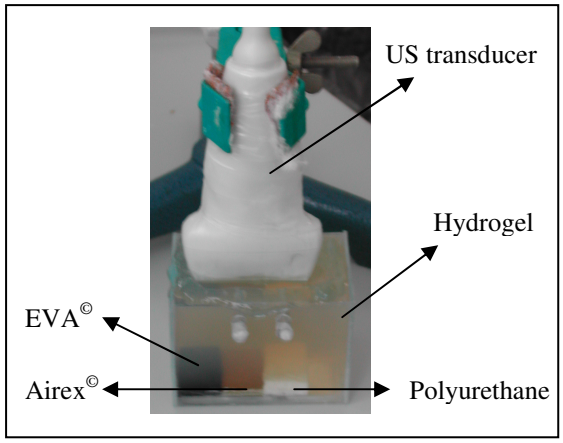

Figure 1: The manufactured phantom coupled with the employed US transducer.

The transducer was connected to a digital ecograph (Megas GPX, Esaote Spa, Florence, Italy), externally linked to a prototype for radiofrequency (RF) analysis (FEMMINA, Fast Echographic Multiparameter Multi Image Novel Apparatus, developed by Florence University), able to get the full raw signal of the probe with no hardware nor software filtering of the ecograph itself [8]. The received signals were digitized at 40 MHz, 16 bits.

The phantom was insonified at eight different transmit frequencies (1.66, 2, 2.5, 3.3, 5, 7.5, 10, 13 MHz) and the corresponding raw data were acquired in sequences of 5 frames and stored in FEMMINA hard disk for further off-line analysis. The number of digitized data points was 3200 for each scan line (approximately matching the phantom depth) and this information was acquired for 180 scan lines in each frame.

Stored raw data were used to reconstruct images through Fortezza software (supplied by Florence University), that was also used to implement new algorithms to properly choose the Region Of Interest (ROI) and to process the corresponding data in various ways. In particular, we used the algorithm reported in figure 2 to select two ROIs, respectively closer (ROI 1) and further (ROI 2) from the sound-absorbant surface. As indicated in figure 3, ROI 1 was composed of 10,000 data points (20 scan lines × 500 points, approximately 0.5 × 1 cm) and it was 750 points (approximately 1.5 cm) far from the sound-absorbant interface. ROI 2 had the same dimensions as ROI 1, but it was 1250 points (approximately 2.5 cm) far from the sound-absorbant material surface.

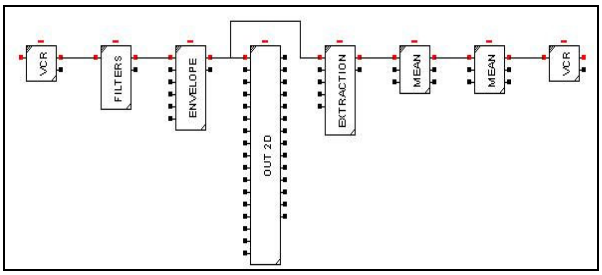

Figure 2: Fortezza algorithm used to select the ROIs and to calculate the mean pixel intensity for each acquired frame.

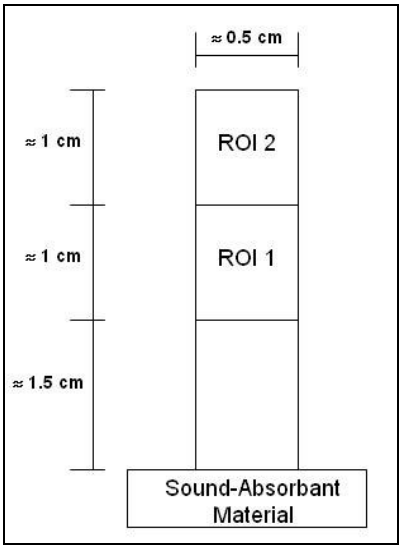

Figure 3: Schematic representation of chosen ROIs.

The mean pixel intensity of the defined ROIs was calculated for each acquired frame, then these values were averaged over the corresponding frame sequence, that had been acquired at costant US frequency.. The resulting values were plotted against the employed US frequency.

It is interesting to note that the algorithm reported in figure 2, when employed to select the ROIs, was set in a different way to that used to calculate the mean pixel intensity. In the first case we just needed a clear ecographic image of the scanned depth, in order to verify the correct transducer placement and to properly locate ROIs; therefore, starting from the RF raw data stored in the module "VCR" in fig. 2, we performed a "highpass" filter (module "FILTERS" in fig. 2) and an envelope with an effective cut frequency (module "ENVELOPE" in fig. 2). In this way we were able to correctly visualize an ecographic image of the investigated phantom section (module "OUT 2D" in fig. 2). In the second situation, that is when we wanted to calculate mean pixel intensity within the selected ROIs, we needed not anymore the ecographic image we used in the previous step and, on the other hand, we did not

ISSN: 1727-1983

want to filter the raw signals in order to avoid the cancellation of important contributions. For the mentioned reasons, in this case, we set the "FILTERS" module as an "all pass" filter (that is it did not perform any operation) and we selected the highest possible cut frequency (20 MHz) in the "ENVELOPE" module, just to take the absolute value of the signal without loosing any frequency content. So it is this "RF raw signal absolute value" that was passed to the "EXTRACTION" module (fig. 2), in which we had previously inserted the spatial coordinates of the chosen ROI: frame by frame, the "EXTRACTION" module selected the data corresponding to the desired ROI and passed them to the "MEAN" modules that calculated the mean value, which was in turn written in a new file ("VCR" module, fig. 2) whose content was then used for statistical analysis and data plotting.

In order to confirm the obtained results, we also performed a different kind of analysis: by employing the algorithms reported in figures 4 and 5, we calculated, directly from RF raw data, the ROI-averaged Fast Fourier Transform (FFT) curves and then we plotted mean single component extracted values against the US transmit frequency.

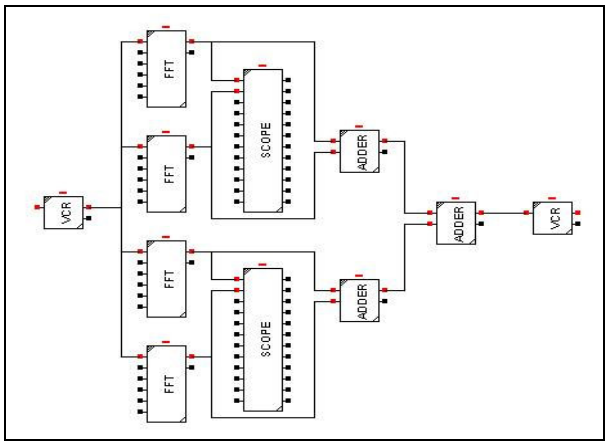

Figure 4: Fortezza algorithm used to calculate and sum the FFT curves for four scan lines of the ROI.

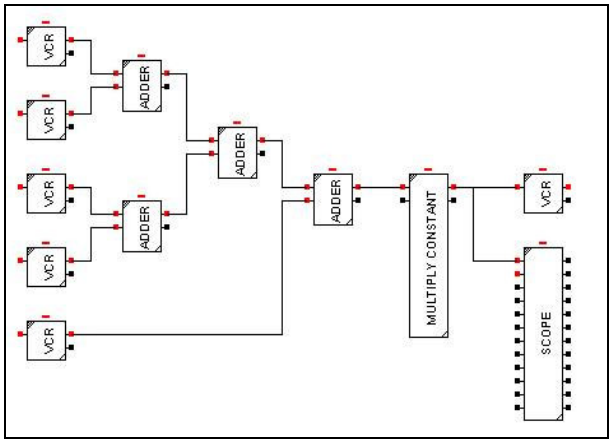

Figure 5: Fortezza algorithm used to obtain the FFT curve averaged over the whole selected ROI.

Here we give a short description of how the algorithms reported in figures 4 and 5 worked. Looking at figure 4, before FFT calculation the raw data corresponding to the defined ROI, selected by means of a 500-point "Hamming" window, were zero-padded to 4096 points to increase the frequency resolution of the spectra ("FFT" modules, fig. 4). FFT was calculated in this way and visualized ("SCOPE" modules, fig. 4) for each scan line of the ROI, then the resulting curves were added ("ADDER" modules, fig. 4) and the finally obtained curve was recorded in a new file ("VCR" module, fig. 4).

The illustrated algorithm processed four scan lines at once, so, since each selected ROI is composed of twenty scan lines, we needed to make use of this algorithm five times for each acquired frame sequence. Afterwards, files produced in this way were processed through the algorithm depicted in figure 5. This algorithm was in fact used to obtain the FFT curve averaged over the whole selected ROI, starting from the curves produced through the algorithm in figure 4 (each initial curve was stored in a different "VCR" module in fig. 5): the curves were summed all together ("ADDER" modules in fig. 5) and divided by 20 (through the "MULTIPLY CONSTANT" module, fig. 5), in order to obtain the mean curve, that was visualized ("SCOPE" module, fig. 5) and stored in a new file ("VCR" module, fig. 5). These files were finally utilized to extract single component FFT values, in turn used for statistical analysis and data plotting. In particular, we extracted the fundamental component backscatter values, we averaged them over the corresponding frame sequence and then we plotted them against the employed US frequency.

Results

Figures 6 and 7 display the relationship between ROI average pixel intensity and US transmit frequency for the three tested materials for both considered ROIs.

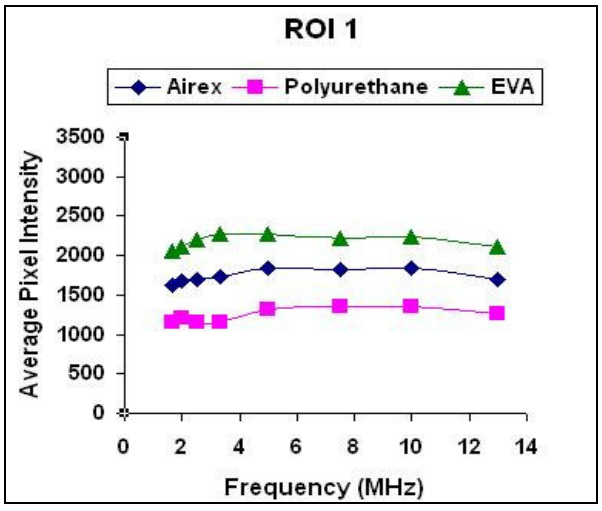

Figure 6: Plot of average pixel intensity versus US transmit frequency in ROI 1.

ISSN: 1727-1983

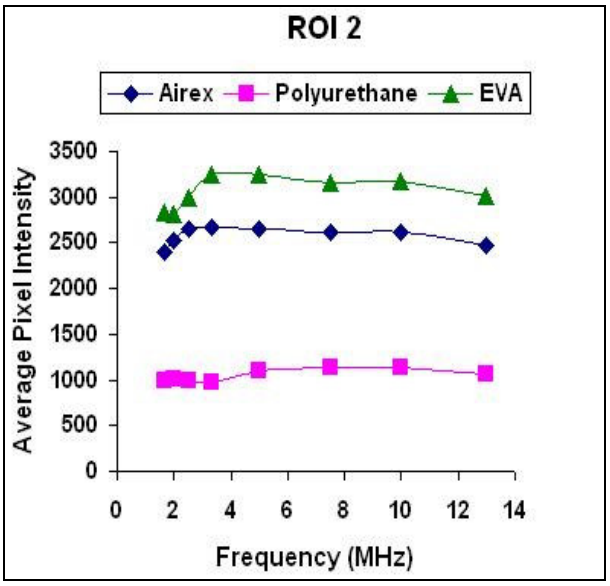

Figure 7: Plot of average pixel intensity versus US transmit frequency in ROI 2.

The minimum intensity was always observed for Polyurethane, in both ROIs and for each employed US frequency. In both figures 6 and 7 it can be observed an almost constant trend for each material in the whole studied frequency range. However, while Polyurethane intensity values remain approximately constant considering ROI 1 or ROI 2, for Airex© and EVA© the average pixel intensity increased in ROI 2 with respect to ROI 1 (i.e. for these materials pixel intensities were higher at bigger distance from the sound-asorbant surface).

Figures 8 and 9 show the behaviour of the backscatter intensities obtained from FFT curves for each one of the studied materials.

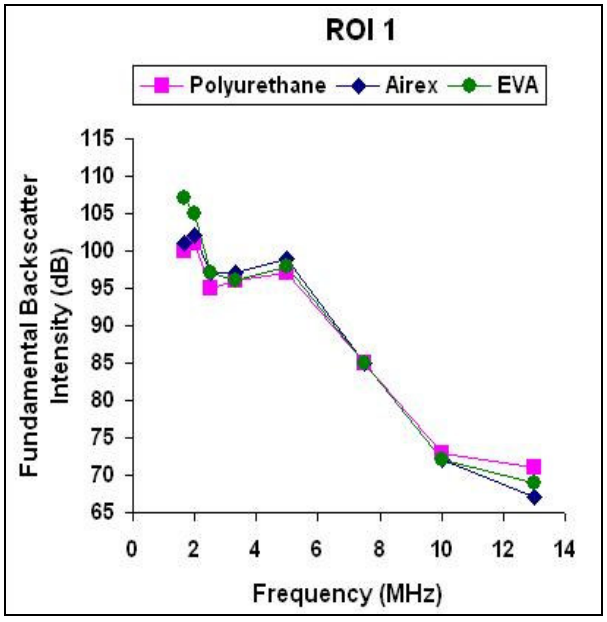

Figure 8: Plot of fundamental backscatter intensity versus US transmit frequency for ROI 1.

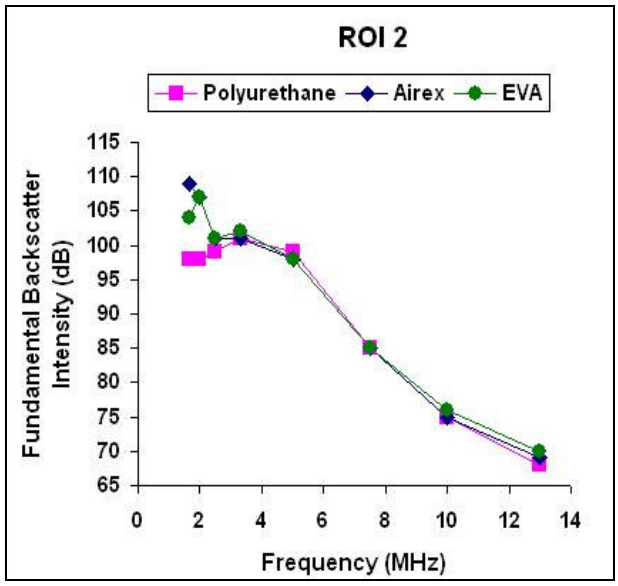

Figure 9: Plot of fundamental backscatter intensity versus US transmit frequency for ROI 2.

Fundamental backscatter intensity values of Airex© and EVA© were higher than the corresponding Polyurethane ones at lower frequencies, while this difference disappeared at higher frequencies. In particular we can observe that the mentioned difference was valuable in ROI 1 only for EVA© and it is not so marked for Airex© (see fig. 8), while in ROI 2 the same divergence was more evident for both materials, especially for Airex© at the lowest employed US frequency (see fig. 9).

Discussion

Airex©, EVA© and Polyurethane showed different sound-absorption grades, that were almost constant for each material in the whole studied frequency range. The best sound-absorption capacity was showed by Polyurethane in both considered ROIs.

It was also possible to note how for Airex© and EVA© the average pixel intensity increased at bigger distance from the sound-absorbant surface (fig. 7). This could probably be due to a higher value of backscatter intensity at lower frequencies for these materials with respect to Polyurethane, indicating a particularly low efficiency of Airex© and EVA© as sound-absorbant materials at low frequencies. This hypothesis was confirmed by the trends of backscatter values extracted from the FFT curves (figures 8 and 9), clearly showing the different behaviour of Polyurethane with respect to the other tested materials.

Conclusions

An important preliminary optimization of the described phantom was presented. Polyurethane showed the best sound-absorbant behaviour among the three tested materials when used to isolate phantom boundaries in ultrasonic applications. Its use, in fact,

ISSN: 1727-1983

allows to minimize the artefacts and to investigate the backscatter properties of different contrast agents without additional aspects due to environmental boundary condition interferences.

The illustrated results were demonstrated employing a wide US frequency range (1.66-13 MHz) and considering distances from the sound-absorbant surface going approximately from 1.5 to 3.5 cm, that represent very suitable dimensions for typical in vitro experiments.

Acknowledgements

We are grateful to ESAOTE Medical systems, in particular to Giuseppe Loliva for his help and availability.

References

[1] FRINKING P.J.A., DE JONG N. (1998): 'Acoustic Modelling of Shell-Encapsulated Gas Bubbles', *Ultrasound Med Biol,* **24**, pp. 523-533

[2] WARD M., WU J., CHIU J.F. (2000): 'Experimental Study of the Effects of Optison Concentration on Sonoporation In Vitro', *Ultrasound Med Biol,* **26,** pp. 1169-1175

[3] PORTER T.R., OBERDORFER J., RAFTER P., LOF J. and XIE F. (2003): 'Microbubble Responses to a Similar Mechanical Index with Different Real-Time Perfusion Imaging Techcniques', *Ultrasound Med. Biol*., **29**, pp. 1187-92

[4] SBOROS V., MORAN C.M., ANDERSON T., PYE S.D., MACLEOD I.C., MILLAR A.M. and MCDICKEN W.N. (2000): 'Evaluation of an Experimental System for the In Vitro Assessment of Ultrasonic Contrast Agents', *Ultrasound Med. Biol*., **26**, pp. 105-11

[5] SBOROS V., MORAN C.M., ANDERSON T., GATZOULIS L., CRITON A., AVERKIOU M., PYE S.D. and MC DICKEN W.N. (2001): 'An In Vitro System for the Study of Ultrasound Contrast Agents Using a Commercial Imaging System', *Phys. Med. Biol*., **46**, pp. 3301-3321

[6] HARRIS C.M. (1991): 'Handbook of Acoustical Measurements and Noise Control", (Acoustical Society of America, Publications)

[7] BAZZOCCHI M. (2001): 'Ecografia', II edition. (Idelson Gnocchi Editor)

[8] SCABIA M., BIAGI E. and MASOTTI L. (2002): 'Hardware and software platform for real-time processing and visualization of echographic radiofrequency signals', *IEEE Trans UFFC*, **49**, pp. 1444-1452

ISSN: 1727-1983